Photonics and Nanostructures – Fundamentals and Applications 30 (2018) 50–56

Contents lists available at ScienceDirect

Photonics and Nanostructures – Fundamentals and Applications

journal homepage: www.elsevier.com/locate/photonics

Invited Paper

Titanium nitride nanoparticles as an alternative platform for plasmonic waveguides in the visible and telecommunication wavelength ranges

V.I. Zakomirnyi[a,b,*], I.L. Rasskazov[c], V.S. Gerasimov[a,d], A.E. Ershov[a,d,e], S.P. Polyutov[a], S.V. Karpov[a,e,f], H. Ågren[a,b]

[a] Institute of Nanotechnology, Spectroscopy and Quantum Chemistry, Siberian Federal University, Krasnoyarsk 660041, Russia
[b] Theoretical Chemistry and Biology, School of Engineering Sciences in Chemistry, Biotechnology and Health, KTH Royal Institute of Technology, 10691 Stockholm, Sweden
[c] The Beckman Institute for Advanced Science and Technology, University of Illinois at Urbana-Champaign, Urbana, IL 61801, USA
[d] Institute of Computational Modeling SB RAS, 660036 Krasnoyarsk, Russia
[e] Siberian State University of Science and Technology, Krasnoyarsk 660014, Russia
[f] Kirensky Institute of Physics, Federal Research Center KSC SB RAS, 660036 Krasnoyarsk, Russia

ARTICLE INFO

Article history:
Received 15 November 2017
Received in revised form 12 March 2018
Accepted 12 April 2018
Available online 17 April 2018

Keywords:
Nanoparticle
Titanium nitride
Surface plasmon polariton
Plasmon waveguide
Refractory plasmonics

ABSTRACT

We propose to utilize titanium nitride (TiN) as an alternative material for linear periodic chains (LPCs) of nanoparticles (NPs) which support surface plasmon polariton (SPP) propagation. Dispersion and transmission properties of LPCs have been examined within the framework of the dipole approximation for NPs with various shapes: spheres, prolate and oblate spheroids. It is shown that LPCs of TiN NPs support high-*Q* eigenmodes for an SPP attenuation that is comparable with LPCs from conventional plasmonic materials such as Au or Ag, with the advantage that the refractory properties and cheap fabrication of TiN nanostructures are more preferable in practical implementations compared to Au and Ag. We show that the SPP decay in TiN LPCs remains almost the same even at extremely high temperatures which is impossible to reach with conventional plasmonic materials. Finally, we show that the bandwidth of TiN LPCs from non-spherical particles can be tuned from the visible to the telecommunication wavelength range by switching the SPP polarization, which is an attractive feature for integrating these structures into modern photonic devices.

1. Introduction

Plasmonic nanoparticles (NPs) are one of the cornerstones of modern science and technology due to an almost uncountable number of applications [1]. The uniqueness of the NPs originates from their ability to support localized surface plasmons (LSPs) which enables strong confinement of electric fields at scales much smaller than the wavelength of the incident radiation. Strong enhancement of local fields is vital for a wide variety of possible applications such as surface enhanced Raman spectroscopy [2], upconversion [3], biomedicine [4] and solar energy harvesting [5].

Arrays of non-touching NPs enable nanoscale electromagnetic energy transfer via propagation of so-called surface plasmon polaritons (SPPs) [6,7] which paves the way for utilization of nanostructures in chemical sensing [8–11], nanoantennas [12,13] and nanosized waveguides [14–19]. Propagation of SPPs is usually considered in 1*D* or 2*D* arrays of NPs from conventional plasmonic materials: Ag [6,15,16,20–24] and Au [17,18,25,26]. Various types of technological aspects such as disorder [15,20], polydispersity [15] impact of the substrate [21,27,28], thermal effects [29] have been thoroughly considered so far. However, high Ohmic losses and consequent overheating of metal NPs lead to strong suppression of the LSPs [30] and, as a result, significant attenuation of the SPP. Moreover, the SPP frequencies lie mostly in the visible or near infrared ranges, while integration with CMOS-compatible devices requires bandwidth of LPCs to lie within the telecommunication wavelength range. These drawbacks make it unlikely that LPCs of plasmonic NPs can be utilized as a tool for efficient guiding of electromagnetic energy over distances of several hundred nanometers for applications in highly integrated optical devices operating below the diffraction limit of light [31].

* Corresponding author at: Institute of Nanotechnology, Spectroscopy and Quantum Chemistry, Siberian Federal University, Krasnoyarsk 660041, Russia.
E-mail address: vi.zakomirnyi@gmail.com (V.I. Zakomirnyi).

https://doi.org/10.1016/j.photonics.2018.04.005
1569-4410/

There are some strategies to deal with strong attenuation of SPPs. For example, utilization of non-spherical NPs can lead to nondecaying propagation of SPPs in LPCs in homogeneous media [32] or to minimization of SPP suppression due to interaction with the dielectric substrate [27]. However, inevitable Ohmic losses in metals and consequent overheating of NPs represent a more complicated problem to deal with. The temperature dependent optical properties of noble metals [30,33–36] imply strong suppression of LSP resonances at high temperatures, which is of crucial importance for SPP propagation. Finally, chemical instability, inability to dynamically adjust optical properties [37] limit successful implementations of Ag and Au LPCs of NPs in photonic devices.

Recent progress in plasmonics, however, indicates a way to overcome drawbacks of conventional noble metals by using so-called alternative plasmonic materials [38,39]. Numerous materials have been benchmarked against conventional Ag and Au in terms of local field enhancement [40] and refractory behavior [41,39,42]. Metal transition nitrides, particularly, titanium nitride (TiN) have been considered as most promising material from this perspective [43–46]. TiN thin films and NPs have a great potential in photodetection [47], solar energy harvesting [48], sustainable energetics [49], nonlinear optics [50,51], and biomedicine [52]. The position of the LSP resonance peak of a single TiN NP lies in the near infrared region [46] which is a vital feature for utilization of TiN NP arrays in photonic devices operating at telecommunication wavelengths [53,54]. Finally, low-cost large area fabrication [55], thermal stability [56] are important advantages of TiN which immediately enable its wide practical implementation.

In this paper, we propose to utilize TiN for waveguiding applications in LPCs of spherical and spheroidal NPs. TiN optical properties provide an opportunity to shift the SPP frequency to telecommunication wavelengths, while the TiN refractory behavior could potentially resolve issues with strong SPP suppression at high temperatures.

2. Model

2.1. Dipole approximation

A substantial part of theoretical and experimental studies of electromagnetic properties of metal nanostructures are based on the dipole approximation (DA) [15,16,21,23,57–62]. This approximation is quite simple yet efficient for accurate description and prediction of optical properties of plasmonic nanostructures. The applicability of DA is, however, strictly limited by the geometry of the structure [63,64]: the distance between the NPs in a periodic array should be significantly larger than the size of the NPs. For example, in the case of nanospheres, the center-to-center distance between neighboring NPs should exceed the NP diameter by the factor of 1.2 and 1.4 for transverse and longitudinal polarization of incident irradiation, respectively, as shown in Ref. [65]. Otherwise, it is necessary to take into account quadrupole [65] or higher order interaction for an adequate description of the electromagnetic properties of such structures.

Although the dipole approximation serves as a well-known approach, extensively described in literature, in this section we provide a general formalism for the convenience of the Readers. Let us consider an LPC of N identical NPs whose centers are located at points $x_n = (n-1)h$, where h is the center-to-center distance, and $n = 1, \ldots, N$. We consider LPCs located in a homogeneous environment with dielectric permittivity ε_h. Assume that the LPC is excited by an external monochromatic electric field $\mathbf{E}_n^{\text{ext}} = \mathbf{E}^{\text{ext}}(x_n)$ (time dependence $\exp(-i\omega t)$ is omitted in all expressions, here ω is the frequency of the incident field). In this case, the dipole moments $\mathbf{d}_n$ induced in each NP are coupled to each other and to the external field via the following coupled dipole equations:

$$\frac{1}{\alpha}\mathbf{d}_n - \sum_{m \neq n}^{N} \hat{G}_{nm}\mathbf{d}_m = \mathbf{E}_n^{ext}, \tag{1}$$

Here α is the polarizability of the NP, $\hat{G}_{nm}$ is the Green's tensor which describes the electric field at x_n point created by a point dipole located at the x_m point. Explicit expressions for the Green's function can be found elsewhere [15,16].

In this paper, we consider three different shapes of NPs: spheres, prolates and oblate spheroids. The quasistatic polarizability of NPs with these shapes is defined by the following expression:

$$\alpha_0 = \frac{4\pi}{V}\frac{\varepsilon_p - \varepsilon_h}{\varepsilon_h + L(\varepsilon_p - \varepsilon_h)}, \tag{2}$$

where V is the volume of the NP, ε_p is the dielectric permittivity of the NP material, L is a static depolarization factor [66].

For NPs with dimensions much smaller than the wavelength of the incident illumination, retardation effects should be taken into account [67,68]. Moreover, a so-called dynamic correction [69] to the polarizability of spheroidal NPs has to be introduced for an adequate description of its electromagnetic properties. Thus, the polarizability α takes the form:

$$\alpha = \alpha_0\left[1 - \frac{k^2}{l_E}D\alpha_0 - i\frac{2k^3}{3}\alpha_0\right]^{-1}, \tag{3}$$

where α_0 is defined by Eq. (2), D is a dynamic geometrical factor [69], $k = \sqrt{\varepsilon_h}\omega/c$ is the wave number, c is the speed of light in a vacuum, l_E is the length of the semiaxis of the NP along which the electric field is applied. Static L and dynamic D depolarization factors for prolate and oblate spheroids can be found with well-known expressions [66,69] which are not provided in this paper. For spherical NPs: $L = 1/3$ and $D = 1$.

Finally, the TiN dielectric permittivity can be described by the Lorentz oscillator model [70]:

$$\varepsilon_p = \varepsilon_\infty - \frac{\omega_p^2}{\omega^2 + i\Gamma_D\omega} + \sum_{j=1}^{2}\frac{\omega_{L,j}^2}{\omega_{0,j}^2 - \omega^2 - i\gamma_j\omega}, \tag{4}$$

where ε_∞ describes high energy interband transitions outside the probed energy spectrum, ω_p is the plasma frequency, Γ_D is the Drude relaxation constant, $\omega_{L,j}^2$, $\omega_{0,j}$, and γ_j describe the Lorentz oscillator strength, energy, and damping, respectively. Temperature-dependent constants entering Eq. (4) are represented in Table 1.

Table 1
Temperature-dependent optical constants for TiN [70].

	23 °C	400 °C	800 °C
ε_∞	7.86981	6.50246	4.87685
ω_p, rad/fs	11.21219	11.37931	11.47047
Γ_D, rad/fs	0.39501	0.56213	0.80521
$\omega_{L,1}$, rad/fs	9.86939	11.76819	15.9342
γ_1, rad/fs	2.15736	1.80793	2.78026
$\omega_{0,1}$, rad/fs	6.18342	6.47208	7.17094
$\omega_{L,2}$, rad/fs	2.28396	4.03393	3.52391
γ_2, rad/fs	1.32176	3.08411	2.76507
$\omega_{0,2}$, rad/fs	3.06892	2.93219	2.79545

2.2. Dispersion properties

Dispersion relations are one of the most important properties which quantify the ability of LPCs from metal NPs to support SPP propagation. There are various approaches to estimate dispersion

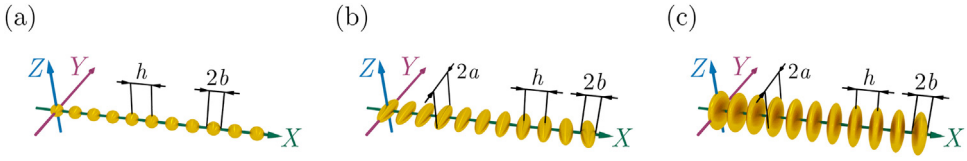

Fig. 1. Schematic representation of LPCs from (a) spheres, (b) prolate spheroids, and (c) oblate spheroids.

relations of finite [57,71,72] and infinite [16,73–79] LPCs, however, in this work, we use an efficient eigendecomposition method [80].

In accordance with the Bloch theorem, the dipole moment and external field in Eq. (1) can be expressed as $\mathbf{d}_n = \mathbf{d} \cdot \exp(iqnh)$ and $\mathbf{E}_n^{ext} = \mathbf{E}^{ext} \cdot \exp(iqnh)$, where q is the eigenvector of the Bloch mode. Thus, Eq. (1) can be written as follows:

$$\left[\frac{1}{\alpha}\hat{I} - \sum_{n=-\infty}^{\infty} \hat{G}_{nm} e^{iqnh}\right] \mathbf{d} = \mathbf{E}^{\text{ext}}. \tag{5}$$

We note that the expression in square brackets has the same dimension as the inverse dipole polarizability α^{-1} of a NP. Thus, according to the eigendecomposition method, it is convenient to characterize the electromagnetic response of the LPC by so-called *effective* polarizability $\tilde{\alpha}$ [80] such that $1/\tilde{\alpha}$ is the eigenvalue of the following operator:

$$\left[\frac{1}{\alpha}\hat{I} - \sum_{n=-\infty}^{\infty} \hat{G}_{nm} e^{iqnh}\right]. \tag{6}$$

Maxima of $\text{Im}[\tilde{\alpha}] = F(\omega, q)$ correspond to LPC resonances, which represent the bandwidth of the LPC, or, in other words, the dispersion relation of the LPC. An essential advantage of the eigendecomposition method is the simultaneous estimation of the LPC eigenmodes and their quality factor [23,80]. Thus, the function$\text{Im}[\tilde{\alpha}] = F(\omega, q)$ provides a complete physical insight into the dispersion relations for LPCs, which is, generally speaking, impossible with other methods considered in the literature [16,57,72–74].

2.3. Transmission properties

While dispersion properties quantify the bandwidth of LPCs, it is useful to calculate the actual damping of the SPP at the end of the waveguide. The most convenient way to do so is to calculate the transmission spectrum of the LPC. Let us assume that the external field $\mathbf{E}^{\text{ext}}$ excites only the first NP in the LPC. This kind of excitation has been used in other works as well [15,21]. Experimentally, it corresponds to an excitation by a near-field optical microscope tip. In this case, the incident field is described as $\mathbf{E}_n^{\text{ext}} = \mathbf{E}^{\text{ext}}\delta_{1n}$, where δ_{mn} is the Kronecker delta. Solution of Eq. (1) with this right-hand side provides the dipole moments $\mathbf{d}_n$ induced on each NP in the LPC. Experimentally, the intensity of the electric field at the end of the LPC $I_N \propto \| \mathbf{d}_N \|^2$ characterizes the attenuation of the SPP. Therefore, the efficiency of the SPP propagation can be described by the following quantity [21]:

$$Q_N = \frac{\|\mathbf{d}_N\|^2}{\|\mathbf{d}_1\|^2}. \tag{7}$$

Thus, we will refer to spectral dependence of Q_N as to the transmission spectrum of the LPC.

3. Results

3.1. LPC geometry

In this work, we study LPCs of NPs with different shapes, as shown in Fig. 1. For spherical NPs, there is no difference in NP orientation with respect to the LPC symmetry axis, however, for spheroidal NPs it is no longer so. We fix the orientation of the spheroids to the following configuration: the shorter semi-axis b of each spheroid is aligned along the X axis, while the longer semi-axis a is orthogonal to the X axis. It is notable, however, that LPCs with spiral-like orientation of spheroidal NPs is a subject for a one-way propagation and a Faraday rotation [81,82], something that is not considered in this work. We set the geometrical parameters of the LPCs to the following constant values: shorter semi-axis $b = 25$ nm and center-to-center distance $h = 75$ nm. These parameters are widely used in numerical simulations of SPP propagation in LPCs from Ag NPs [6,7,14,21,23,57,63]. The longer semi-axis a has been changed for spheroids with different aspect ratios b/a. DA is adequate for LPCs with these geometric parameters [63]. Finally, the dielectric permittivity of the host medium was set to $\varepsilon_h = 2.25$. In a real experiment, this kind of surrounding can be achieved by depositing NPs on a quartz substrate and subsequently covering them by a poly(methyl methacrylate) superstrate [83]. Although it is obvious that the optical properties of surrounding medium are temperature-dependent, we assume that ε_h is constant for the considered frequencies and temperatures [84].

3.2. Dispersion properties

Let us start with the LPC dispersion properties. We plot $\log[\text{Im}(\tilde{\alpha})]$ vs. the SPP frequency ω and the eigenmode wavevector q. According to the eigendecomposition method, high values of $\text{Im}(\tilde{\alpha})$ correspond to high Q-factor eigenmodes. While the summation in Eq. (6) runs to infinity, we consider finite, but sufficiently long, LPCs namely, $N = 1000$ NPs. We begin with LPCs from spherical NPs, the dispersion relations of which are depicted in the first column of Figs. 2 and 3. It can be seen that the SPPs effectively propagate for both longitudinal (X) and transverse (Y) polarizations at $\omega \approx 2.5$–3.5 rad/fs frequencies. However, the branch which corresponds to highest values of $\text{Im}(\tilde{\alpha})$ has quite small slope, which corresponds to a low group velocity of SPPs at this spectral range.

It is well known, however, that the utilization of non-spherical NPs in LPCs significantly increases SPP group velocity [16,72] and simultaneously minimizes the suppression of the SPP [32]. Thus, it is of interest to consider dispersion relations of LPCs from prolate and oblate spheroids with different values of the aspect ratio b/a. It can be seen from Figs. 2 and 3, that in the case of longitudinal polarization, the overall shape of the dispersion branches is almost the same as for LPCs from spherical NPs. This kind of behavior is explained by a negligible difference of the depolarization factors L for different shapes of the NPs with the same values of the shorter semi-axis b which is parallel to polarization of SPP. However, for oblate spheroids with $b/a = 0.4$, the Q-factor of the eigenmodes near the light line $\omega = q/c$ is significantly larger.

In the case of transverse polarization, values of $\log[\text{Im}(\tilde{\alpha})]$ substantially increase, especially for $\omega \approx 1.5$–2.5 rad/fs spectral range

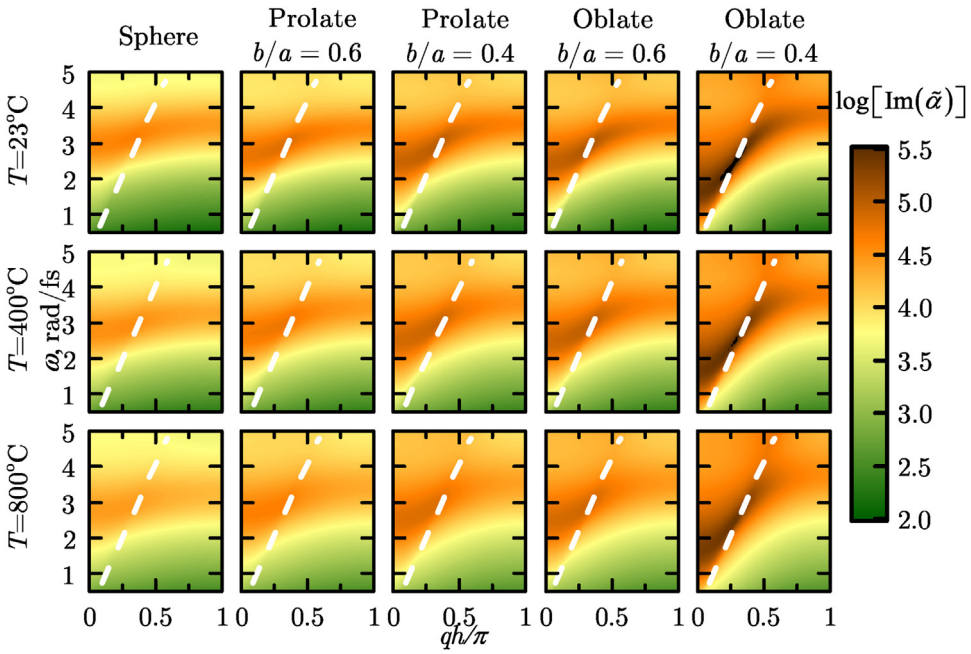

Fig. 2. Dispersion relations for LPCs from spherical and spheroidal particles at different temperatures for longitudinal (X) polarization of SPPs. White dashed line represents the light line $\omega = q/c$.

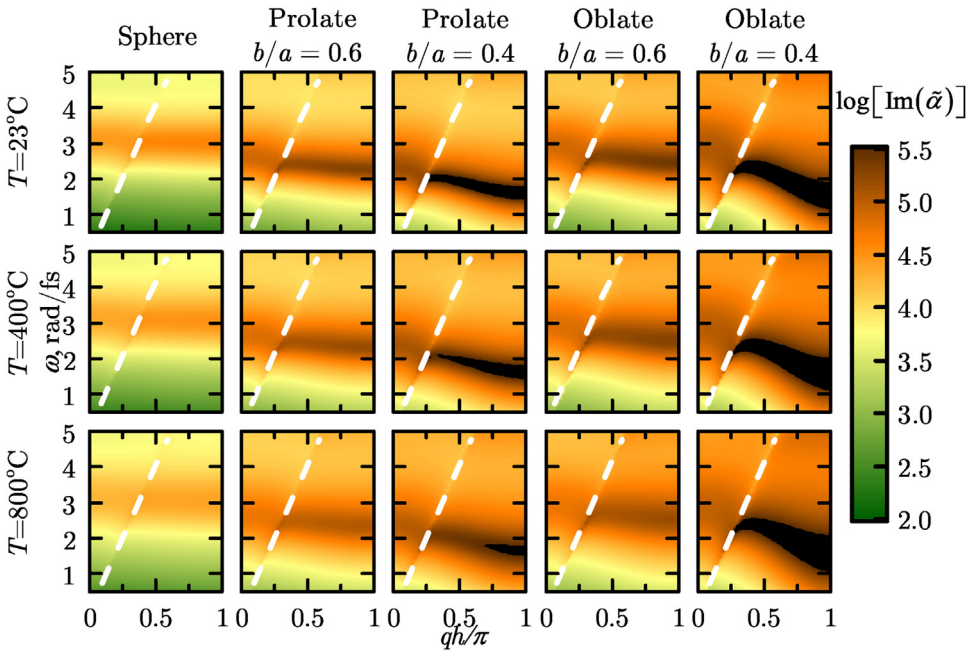

Fig. 3. The same as in Fig. 2, but for transverse (Y) polarization of SPPs.

for LPCs from prolate and oblate spheroids with $b/a = 0.4$. Dispersion branches for LPCs from oblate spheroids have even greater slopes as compared with LPCs from prolate spheroids with the same values of b/a. In addition, the frequency of the eigenmodes decreases to $\omega \approx 1$–2 rad/fs, which basically corresponds to the telecommunication wavelength range. Moreover, the bandwidth of the LPC significantly increases in this case. Finally, the dispersion branch acquires a significant negative slope, which leads to an increase of the SPP group velocity and to anti-parallel propagation of the group and phase velocities of the SPP. Propagation of transversely polarized SPPs with anti-parallel group and phase velocities has been explained in detail in Refs [7,16,23]. Nonetheless, it is worthwhile to mention that the negative slope of the dispersion curve is not a direct proof that LPCs are metamaterials with negative refraction.

Suppression of SPP due to overheating of LPCs is a crucial drawback [29] which significantly limits the widespread use of silver and gold NPs for waveguiding applications. In this sense, TiN is advantageous due to its refractory properties [41]. It can be seen from Figs. 2 and 3 that the dispersion relations of the LPCs of TiN NPs remain almost intact even at $T = 800\,^{\circ}$C. The eigenmode quality factor inevitably decreases at high temperature, however, the suppression of SPPs is much lower than one could expect for a conventional plasmonic materials. We note that in this work LPCs are assumed to be uniformly heated, which represents the most

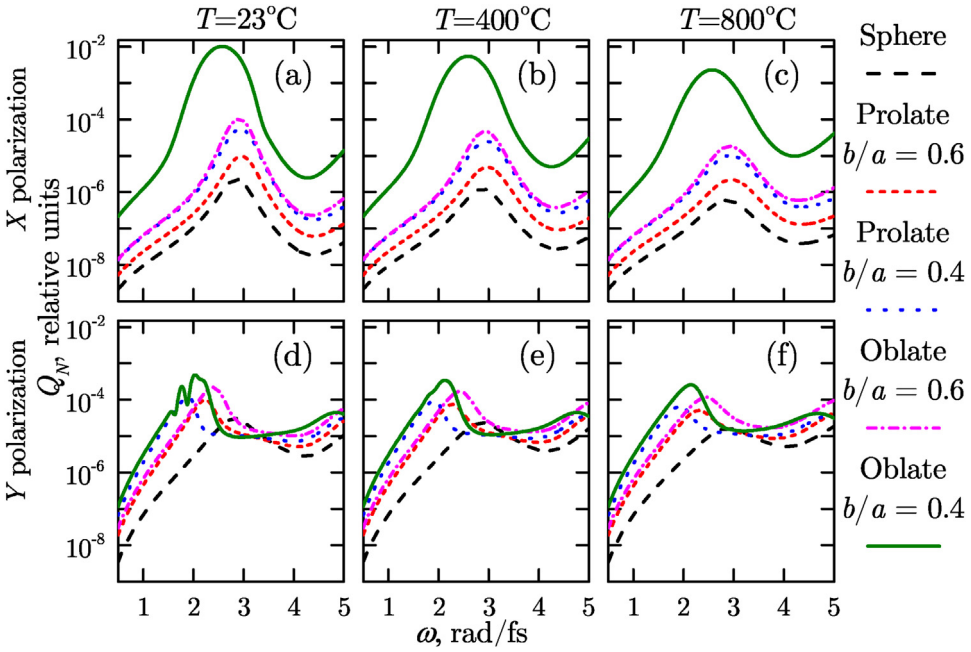

Fig. 4. Transmission spectra of LPCs from TiN NPs of various shapes for *X* polarization (a)–(c) and for *Y* polarization (d)–(f) of the SPPs, and at different temperatures: (a) and (d) $T = 23\,^{\circ}C$; (b) and (e) $T = 400\,^{\circ}C$; (c) and (f) $T = 800\,^{\circ}C$.

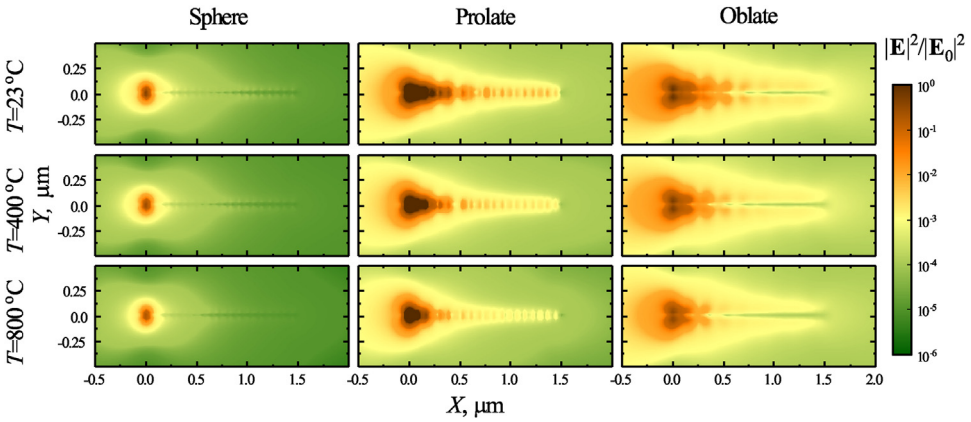

Fig. 5. Electric field localization $|\mathbf{E}|^2/|\mathbf{E}_0|^2$ of LPCs from spherical, prolate and oblate (with $b/a = 0.4$ for both type of spheroids) TiN NPs for *Y* polarization of the SPP at different temperatures. The frequencies were taken in accordance with the maximum values of Q_N from Fig. 4. Excitation is at the NP on the left.

extreme case of overheating. In practice, only three neighboring NPs experience the most pronounced heating in the case of local SPP excitation [29].

One of the exciting features that can be observed from a careful analysis of Figs. 2 and 3 is that the SPP bandwidth (spectral range which corresponds to high-*Q* eigenmodes) significantly changes from longitudinal to transverse polarization for LPCs made of spheroids with $b/a = 0.4$. For longitudinal polarization, the LPC bandwidth corresponds to the visible wavelength range, while for transverse polarization it lies in telecom. Thus, TiN LPCs can simultaneously operate at two important wavelength ranges, which makes it possible to utilize such LPCs as a hybrid photonic interconnector.

3.3. Transmission properties

We turn to the transmission properties of the LPCs by considering SPP propagation in short LPCs from $N = 20$ NPs. It can be seen from Fig. 4 that, indeed, the LPC bandwidth can be adjusted by switching the SPP polarization from longitudinal to transverse value. Moreover, Q_N slightly decrease at high temperatures, which is of crucial importance for waveguiding applications of LPCs. As it may be expected, the most efficient propagation of SPPs takes place in LPCs of oblate spheroids with small aspect ratios e.g. $b/a = 0.4$, which is consistent with results reported in Refs [32,72].

3.4. Electric field localization

Finally, get another attractive property of LPCs is the ability to confine the electromagnetic energy at scales much smaller than the wavelength of the propagating excitation. This feature differs the LPCs from classic strip waveguides [85], the transverse dimensions of which are usually comparable or several times larger that the wavelength of propagating signal. A tight localization of the electromagnetic field near the LPCs makes it possible to arrange several LPCs in a close vicinity to each other without a risk of overlapping of SPPs propagating in neighboring LPCs, which cannot be achieved in strip waveguides.

Fig. 5 shows temperature-dependent intensity plots $|\mathbf{E}|^2/|\mathbf{E}_0|^2$ for LPCs from TiN NPs at 10 nm distance from top-most points of the

NPs. The frequencies ω of SPPs were chosen to match the maximum values of Q_N for Y polarization of the SPPs from Fig. 4(d–f). It can be seen that in the case of spherical NPs, the electric field is tightly localized near the first excited NP and rapidly attenuates along the LPC. The most efficient localization of the electric field is observed in the case of prolate spheroids, moreover, as it can be seen from Fig. 5, the field is confined within ≈500 nm spatial region near the LPC, which is several times smaller than the wavelength of the SPP. The intensity $|\mathbf{E}|^2/|\mathbf{E}_0|^2$ pattern looks completely different for LPCs from oblate spheroids due to the high values of the local field at the tips of the oblate spheroids. Finally, due to the refractory behavior, electric field confinement of LPCs from TiN NPs remains almost the same even at elevated temperatures.

4. Conclusion

To conclude, we have shown that TiN is a promising alternative material that can be used in periodic arrays of nanoparticles to support efficient propagation of surface plasmon polaritons. The bandwidth of linear periodic chains from TiN nanoparticles can be tailored from the visible range to telecom through varying the nanoparticle shape and polarization of the surface plasmon polaritons. Despite inevitable Ohmic losses and overheating of the nanoparticles, the attenuation of the surface plasmon polaritons remains almost the same even at high temperatures due to advantageous TiN refractory properties. Along with cheap methods of large-area fabrication of TiN nanoparticles, these features make TiN a promising plasmonic material for waveguiding applications using linear periodic chains of the nanoparticles.

Acknowledgments

This work was supported by the RF Ministry of Education and Science, the State contract with Siberian Federal University for scientific research in 2017–2019 and SB RAS Program No II.2P (0358-2015-0010).

References

[1] S.A. Maier, Plasmonics: Fundamentals and Applications, Springer US, Boston, MA, 2007.
[2] J.-F. Li, Y.-J. Zhang, S.-Y. Ding, R. Panneerselvam, Z.-Q. Tian, Core–shell nanoparticle-enhanced Raman spectroscopy, Chem. Rev. 117 (2017) 5002–5069.
[3] D.M. Wu, A. García-Etxarri, A. Salleo, J.A. Dionne, Plasmon-enhanced upconversion, J. Phys. Chem. Lett. 5 (2014) 4020–4031.
[4] N.S. Abadeer, C.J. Murphy, Recent progress in cancer thermal therapy using gold nanoparticles, J. Phys. Chem. C 120 (2016) 4691–4716.
[5] J. Li, S.K. Cushing, F. Meng, T.R. Senty, A.D. Bristow, N. Wu, Plasmon-induced resonance energy transfer for solar energy conversion, Nat. Photonics 9 (2015) 601–607.
[6] M. Quinten, A. Leitner, J.R. Krenn, F.R. Aussenegg, Electromagnetic energy transport via linear chains of silver nanoparticles, Opt. Lett. 23 (1998) 1331.
[7] S.A. Maier, P.G. Kik, H.A. Atwater, S. Meltzer, E. Harel, B.E. Koel, A.A. Requicha, Local detection of electromagnetic energy transport below the diffraction limit in metal nanoparticle plasmon waveguides, Nat. Mater. 2 (2003) 229–232.
[8] M.E. Stewart, C.R. Anderton, L.B. Thompson, J. Maria, S.K. Gray, J.A. Rogers, R.G. Nuzzo, Nanostructured plasmonic sensors, Chem. Rev. 108 (2008) 494–521.
[9] A.B. Evlyukhin, S.I. Bozhevolnyi, A. Pors, M.G. Nielsen, I.P. Radko, M. Willatzen, O. Albrektsen, Detuned electrical dipoles for plasmonic sensing, Nano Lett. 10 (2010) 4571–4577.
[10] G. Li, X. Li, M. Yang, M.-M. Chen, L.-C. Chen, X.-L. Xiong, A gold nanoparticles enhanced surface plasmon resonance immunosensor for highly sensitive detection of ischemia-modified albumin, Sensors 13 (2013) 12794–12803.
[11] V.G. Kravets, F. Schedin, R. Jalil, L. Britnell, R.V. Gorbachev, D. Ansell, B. Thackray, K.S. Novoselov, A.K. Geim, A.V. Kabashin, A.N. Grigorenko, Singular phase nano-optics in plasmonic metamaterials for label-free single-molecule detection, Nat. Mater. 12 (2013) 304–309.
[12] A.F. Koenderink, Plasmon nanoparticle array waveguides for single photon and single plasmon sources, Nano Lett. 9 (2009) 4228–4233.
[13] J. Munárriz, A.V. Malyshev, V.A. Malyshev, J. Knoester, Optical nanoantennas with tunable radiation patterns, Nano Lett. 13 (2013) 444–450.
[14] M.L. Brongersma, J.W. Hartman, H.A. Atwater, Electromagnetic energy transfer and switching in nanoparticle chain arrays below the diffraction limit, Phys. Rev. B 62 (2000) R16356–R16359.
[15] V.A. Markel, A.K. Sarychev, Propagation of surface plasmons in ordered and disordered chains of metal nanospheres, Phys. Rev. B 75 (2007) 085426.
[16] A.A. Govyadinov, V.A. Markel, From slow to superluminal propagation: dispersive properties of surface plasmon polaritons in linear chains of metallic nanospheroids, Phys. Rev. B 78 (2008) 035403.
[17] M. Février, P. Gogol, A. Aassime, R. Mégy, C. Delacour, A. Chelnokov, A. Apuzzo, S. Blaize, J.-m. Lourtioz, B. Dagens, Giant coupling effect between metal nanoparticle chain and optical waveguide, Nano Lett. 12 (2012) 1032–1037.
[18] A. Apuzzo, M. Février, R. Salas-Montiel, A. Bruyant, A. Chelnokov, G. Lérondel, B. Dagens, S. Blaize, Observation of near-field dipolar interactions involved in a metal nanoparticle chain waveguide, Nano Lett. 13 (2013) 1000–1006.
[19] W. Aroua, F. AbdelMalek, A.A. Kamli, Optical diode based on plasmonic nanosphere chains, Opt. Commun. 332 (2014) 25–30.
[20] F. Rüting, Plasmons in disordered nanoparticle chains: localization and transport, Phys. Rev. B 83 (2011) 115447.
[21] P.J. Compaijen, V.A. Malyshev, J. Knoester, Surface-mediated light transmission in metal nanoparticle chains, Phys. Rev. B 87 (2013) 205437.
[22] D. Solis, A. Paul, J. Olson, L.S. Slaughter, P. Swanglap, W.-S. Chang, S. Link, Turning the corner: efficient energy transfer in bent plasmonic nanoparticle chain waveguides, Nano Lett. 13 (2013) 4779–4784.
[23] P.J. Compaijen, V.A. Malyshev, J. Knoester, Engineering plasmon dispersion relations: hybrid nanoparticle chain-substrate plasmon polaritons, Opt. Express 23 (2015) 2280.
[24] G. Song, W. Zhang, Electromagnetic field propagation in the one-dimensional silver nanoparticle dimer chains: hotspots and energy transport, Plasmonics 12 (2017) 179–184.
[25] S.A. Maier, P.G. Kik, H.A. Atwater, Observation of coupled plasmon-polariton modes in Au nanoparticle chain waveguides of different lengths: estimation of waveguide loss, Appl. Phys. Lett. 81 (2002) 1714.
[26] S.A. Maier, M.L. Brongersma, P.G. Kik, H.A. Atwater, Observation of near-field coupling in metal nanoparticle chains using far-field polarization spectroscopy, Phys. Rev. B 65 (2002) 193408.
[27] I.L. Rasskazov, S.V. Karpov, G.Y. Panasyuk, V.A. Markel, Overcoming the adverse effects of substrate on the waveguiding properties of plasmonic nanoparticle chains, J. Appl. Phys. 119 (2016).
[28] D. Szafranek, Y. Leviatan, A source-model technique for analysis of waveguiding across an array of arbitrary smooth cylinders partially buried in a penetrable substrate, IEEE Trans. Antennas Propag. 65 (2017) 2748–2753.
[29] A.E. Ershov, V.S. Gerasimov, A.P. Gavrilyuk, S.V. Karpov, V.I. Zakomirnyi, I.L. Rasskazov, S.P. Polyutov, Thermal limiting effects in optical plasmonic waveguides, J. Quant. Spectrosc. Radiat. Transf. 191 (2017) 1–6.
[30] V.S. Gerasimov, A.E. Ershov, A.P. Gavrilyuk, S.V. Karpov, H. Ågren, S.P. Polyutov, Suppression of surface plasmon resonance in Au nanoparticles upon transition to the liquid state, Opt. Express 24 (2016) 26851.
[31] N. Kinsey, M. Ferrera, V.M. Shalaev, A. Boltasseva, Examining nanophotonics for integrated hybrid systems: a review of plasmonic interconnects and modulators using traditional and alternative materials [Invited], J. Opt. Soc. Am. B 32 (2015) 121.
[32] I.L. Rasskazov, S.V. Karpov, V.A. Markel, Nondecaying surface plasmon polaritons in linear chains of silver nanospheroids, Opt. Lett. 38 (2013) 4743.
[33] H. Reddy, U. Guler, A.V. Kildishev, A. Boltasseva, V.M. Shalaev, Temperature-dependent optical properties of gold thin films, Opt. Mater. Express 6 (2016) 2776.
[34] A.V. Kalenskii, A.A. Zvekov, A.P. Nikitin, Influence of temperature on optical properties of silver nanoparticle-transparent matrix composites, J. Appl. Spectrosc. 83 (2017) 1020–1025.
[35] A.V. Kalenskii, A.A. Zvekov, M.V. Anan'eva, A.P. Nikitin, B.P. Aduev, The influence of temperature on the optical properties of gold nanoparticles, Opt. Spectrosc. 122 (2017) 402–409.
[36] H. Reddy, U. Guler, K. Chaudhuri, A. Dutta, A.V. Kildishev, V.M. Shalaev, A. Boltasseva, Temperature-dependent optical properties of single crystalline and polycrystalline silver thin films, ACS Photonics 4 (2017) 1083–1091.
[37] Y. Tang, M. Ouyang, Tailoring properties and functionalities of metal nanoparticles through crystallinity engineering, Nat. Mater. 6 (2007) 754–759.
[38] P. West, S. Ishii, G. Naik, N. Emani, V. Shalaev, A. Boltasseva, Searching for better plasmonic materials, Laser Photonics Rev. 4 (2010) 795–808.
[39] G.V. Naik, V.M. Shalaev, A. Boltasseva, Alternative plasmonic materials: beyond gold and silver, Adv. Mater. 25 (2013) 3264–3294.
[40] U. Guler, G.V. Naik, A. Boltasseva, V.M. Shalaev, A.V. Kildishev, Performance analysis of nitride alternative plasmonic materials for localized surface plasmon applications, Appl. Phys. B 107 (2012) 285–291.
[41] U. Guler, A. Boltasseva, V.M. Shalaev, Refractory plasmonics, Science 344 (2014) 263–264.
[42] A. Lalisse, G. Tessier, J. Plain, G. Baffou, Quantifying the efficiency of plasmonic materials for near-field enhancement and photothermal conversion, J. Phys. Chem. C 119 (2015) 25518–25528.
[43] G.V. Naik, J.L. Schroeder, X. Ni, A.V. Kildishev, T.D. Sands, A. Boltasseva, Titanium nitride as a plasmonic material for visible and near-infrared wavelengths, Opt. Mater. Express 2 (2012) 478.
[44] S. Prayakarao, S. Robbins, N. Kinsey, A. Boltasseva, V.M. Shalaev, U.B. Wiesner, C.E. Bonner, R. Hussain, N. Noginova, M.A. Noginov, Gyroidal titanium nitride as nonmetallic metamaterial, Opt. Mater. Express 5 (2015) 1316.

[45] C.M. Zgrabik, E.L. Hu, Optimization of sputtered titanium nitride as a tunable metal for plasmonic applications, Opt. Mater. Express 5 (2015) 2786.
[46] U. Guler, V.M. Shalaev, A. Boltasseva, Nanoparticle plasmonics: going practical with transition metal nitrides, Mater. Today 18 (2015) 227–237.
[47] A.A. Hussain, B. Sharma, T. Barman, A.R. Pal, Self-powered broadband photodetector using plasmonic titanium nitride, ACS Appl. Mater. Interfaces 8 (2016) 4258–4265.
[48] N. Venugopal, V.S. Gerasimov, A.E. Ershov, S.V. Karpov, S.P. Polyutov, Titanium nitride as light trapping plasmonic material in silicon solar cell, Opt. Mater. 72 (2017) 397–402.
[49] M. Kaur, S. Ishii, S.L. Shinde, T. Nagao, All-ceramic microfibrous solar steam generator: TiN plasmonic nanoparticle-loaded transparent microfibers, ACS Sustain. Chem. Eng. 5 (2017) 8523–8528.
[50] L. Gui, S. Bagheri, N. Strohfeldt, M. Hentschel, C.M. Zgrabik, B. Metzger, H. Linnenbank, E.L. Hu, H. Giessen, Nonlinear refractory plasmonics with titanium nitride nanoantennas, Nano Lett. 16 (2016) 5708–5713.
[51] S.S. Kharintsev, A.V. Kharitonov, S.K. Saikin, A.M. Alekseev, S.G. Kazarian, Nonlinear Raman effects enhanced by surface plasmon excitation in planar refractory nanoantennas, Nano Lett. 17 (2017) 5533–5539.
[52] W. He, K. Ai, C. Jiang, Y. Li, X. Song, L. Lu, Plasmonic titanium nitride nanoparticles for in vivo photoacoustic tomography imaging and photothermal cancer therapy, Biomaterials 132 (2017) 37–47.
[53] J.A. Briggs, G.V. Naik, T.A. Petach, B.K. Baum, D. Goldhaber-Gordon, J.A. Dionne, Fully CMOS-compatible titanium nitride nanoantennas, Appl. Phys. Lett. 108 (2016) 051110.
[54] V.I. Zakomirnyi, I.L. Rasskazov, V.S. Gerasimov, A.E. Ershov, S.P. Polyutov, S.V. Karpov, Refractory titanium nitride two-dimensional structures with extremely narrow surface lattice resonances at telecommunication wavelengths, Appl. Phys. Lett. 111 (2017) 123107.
[55] S. Bagheri, C.M. Zgrabik, T. Gissibl, A. Tittl, F. Sterl, R. Walter, S. De Zuani, A. Berrier, T. Stauden, G. Richter, E.L. Hu, H. Giessen, Large-area fabrication of TiN nanoantenna arrays for refractory plasmonics in the mid-infrared by femtosecond direct laser writing and interference lithography [Invited], Opt. Mater. Express 5 (2015) 2625.
[56] U. Guler, J.C. Ndukaife, G.V. Naik, A.G.A. Nnanna, A.V. Kildishev, V.M. Shalaev, A. Boltasseva, Local heating with lithographically fabricated plasmonic titanium nitride nanoparticles, Nano Lett. 13 (2013) 6078–6083.
[57] W.H. Weber, G.W. Ford, Propagation of optical excitations by dipolar interactions in metal nanoparticle chains, Phys. Rev. B 70 (2004) 125429.
[58] A. Alù, N. Engheta, Theory of linear chains of metamaterial/plasmonic particles as subdiffraction optical nanotransmission lines, Phys. Rev. B 74 (2006) 205436.
[59] N. Esteves-López, H.M. Pastawski, R.A. Bustos-Marún, Plasmonic graded-chains as deep-subwavelength light concentrators, J. Phys.: Condens. Matter 27 (2015) 125301.
[60] Y. Mazor, Y. Hadad, B.Z. Steinberg, Planar one-way guiding in periodic particle arrays with asymmetric unit cell and general group-symmetry considerations, Phys. Rev. B 92 (2015) 125129.
[61] N.A. Pike, D. Stroud, Faraday rotation, band splitting, and one-way propagation of plasmon waves on a nanoparticle chain, J. Appl. Phys. 119 (2016).
[62] N. Mahi, G. Lévêque, O. Saison, J. Marae-Djouda, R. Caputo, A. Gontier, T. Maurer, P.-M. Adam, B. Bouhafs, A. Akjouj, In depth investigation of lattice plasmon modes in substrate-supported gratings of metal monomers and dimers, J. Phys. Chem. C 121 (2017) 2388–2401.
[63] S.Y. Park, D. Stroud, Surface-plasmon dispersion relations in chains of metallic nanoparticles: an exact quasistatic calculation, Phys. Rev. B 69 (2004) 125418.
[64] B. Rolly, N. Bonod, B. Stout, Dispersion relations in metal nanoparticle chains: necessity of the multipole approach, J. Opt. Soc. Am. B 29 (2012) 1012.
[65] A. Alù, N. Engheta, Guided propagation along quadrupolar chains of plasmonic nanoparticles, Phys. Rev. B 79 (2009) 235412.
[66] C.F. Bohren, D.R. Huffman, Absorption and Scattering of Light by Small Particles, Wiley-VCH Verlag GmbH, Weinheim, Germany, 1998.
[67] B.T. Draine, The discrete-dipole approximation and its application to interstellar graphite grains, Astrophys. J. 333 (1988) 848.
[68] J.D. Jackson, Classical Electrodynamics, 3rd ed., John Wiley & Sons, Inc., 1999.
[69] A. Moroz, Depolarization field of spheroidal particles, J. Opt. Soc. Am. B 26 (2009) 517.
[70] H. Reddy, U. Guler, Z. Kudyshev, A.V. Kildishev, V.M. Shalaev, A. Boltasseva, Temperature-dependent optical properties of plasmonic titanium nitride thin films, ACS Photonics 4 (2017) 1413–1420.
[71] B. Willingham, S. Link, Energy transport in metal nanoparticle chains via sub-radiant plasmon modes, Opt. Express 19 (2011) 6450.
[72] I.L. Rasskazov, S.V. Karpov, V.A. Markel, Waveguiding properties of short linear chains of nonspherical metal nanoparticles, J. Opt. Soc. Am. B 31 (2014) 2981–2989.
[73] A.F. Koenderink, A. Polman, Complex response and polariton-like dispersion splitting in periodic metal nanoparticle chains, Phys. Rev. B 74 (2006) 033402.
[74] I.B. Udagedara, I.D. Rukhlenko, M. Premaratne, Surface plasmon-polariton propagation in piecewise linear chains of composite nanospheres: the role of optical gain and chain layout, Opt. Express 19 (2011) 19973.
[75] M. Conforti, M. Guasoni, Dispersive properties of linear chains of lossy metal nanoparticles, J. Opt. Soc. Am. B 27 (2010) 1576.
[76] M. Guasoni, M. Conforti, Complex dispersion relation of a double chain of lossy metal nanoparticles, J. Opt. Soc. Am. B 28 (2011) 1019.
[77] W.A. Jacak, Exact solution for velocity of plasmon-polariton in metallic nano-chain, Opt. Express 22 (2014) 18958.
[78] C.A. Downing, E. Mariani, G. Weick, Retardation effects on the dispersion and propagation of plasmons in metallic nanoparticle chains, J. Phys.: Condens. Matter 30 (2018) 025301.
[79] P.J. Compaijen, V.A. Malyshev, J. Knoester, Time-dependent transport of a localized surface plasmon through a linear array of metal nanoparticles: precursor and normal mode contributions, Phys. Rev. B 97 (2018) 085428.
[80] K.H. Fung, C.T. Chan, Plasmonic modes in periodic metal nanoparticle chains: a direct dynamic eigenmode analysis, Opt. Lett. 32 (2007) 973.
[81] Y. Hadad, B.Z. Steinberg, Magnetized spiral chains of plasmonic ellipsoids for one-way optical waveguides, Phys. Rev. Lett. 105 (2010) 233904.
[82] Y. Hadad, Y. Mazor, B.Z. Steinberg, Green's function theory for one-way particle chains, Phys. Rev. B 87 (2013) 035130.
[83] D. Khlopin, F. Laux, W.P. Wardley, J. Martin, G.A. Wurtz, J. Plain, N. Bonod, A.V. Zayats, W. Dickson, D. Gérard, Lattice modes and plasmonic linewidth engineering in gold and aluminum nanoparticle arrays, J. Opt. Soc. Am. B 34 (2017) 691.
[84] J. Gong, R. Dai, Z. Wang, C. Zhang, X. Yuan, Z. Zhang, Temperature dependent optical constants for SiO_2 film on Si substrate by ellipsometry, Mater. Res. Express 4 (2017) 085005.
[85] N. Kinsey, M. Ferrera, G.V. Naik, V.E. Babicheva, V.M. Shalaev, A. Boltasseva, Experimental demonstration of titanium nitride plasmonic interconnects, Opt. Express 22 (2014) 12238.